AD_____

Award Number:
W81XWH-11-1-0090

TITLE: Simulated Optimization of Brachytherapy for the Treatment of Breast Cancer

PRINCIPAL INVESTIGATOR:
Miriam Graf

CONTRACTING ORGANIZATION: University of California, San Diego
La Jolla CA 92093

REPORT DATE: March 2014

TYPE OF REPORT: Final

PREPARED FOR: U.S. Army Medical Research and Materiel Command
Fort Detrick, Maryland 21702-5012

REPORT DOCUMENTATION PAGE

Form Approved
OMB No. 0704-0188

1. REPORT DATE	2. REPORT TYPE	3. DATES COVERED
March 2014	Final	15Dec2010 - 14Dec2013

4. TITLE AND SUBTITLE
Simulated Optimization of Brachytherapy for the Treatment of Breast Cancer

5a. CONTRACT NUMBER

5b. GRANT NUMBER
W81XWH-11-1-0090

5c. PROGRAM ELEMENT NUMBER

6. AUTHOR(S)
Miriam Graf

E-Mail: mgraf@physics.ucsd.edu

5d. PROJECT NUMBER

5e. TASK NUMBER

5f. WORK UNIT NUMBER

7. PERFORMING ORGANIZATION NAME(S) AND ADDRESS(ES)
University of California, San Diego
La Jolla, California 92093

8. PERFORMING ORGANIZATION REPORT NUMBER

9. SPONSORING / MONITORING AGENCY NAME(S) AND ADDRESS(ES)
U.S. Army Medical Research and Materiel Command
Fort Detrick, Maryland 21702-5012

10. SPONSOR/MONITOR'S ACRONYM(S)

11. SPONSOR/MONITOR'S REPORT NUMBER(S)

12. DISTRIBUTION / AVAILABILITY STATEMENT
Approved for Public Release; Distribution Unlimited

13. SUPPLEMENTARY NOTES

14. ABSTRACT
This project's dual objectives are the preparation of the PI for a career in breast cancer research and the design of a system of computer-base simulations capable of evaluating the effectiveness of various methods of breast cancer brachytherapy treatments both in general and for each individual patient for use in clinical decision-making. An initial simple tissue and device model developed using the finite element software ABAQUS was expounded upon to create a more complex model utilizing tissue inhomogeneity to inform both the FEM and Monte Carlo models. Modeled devices were simulated in a detailed patient model in the FEM software in order to create the geometry for the Monte Carlo calculation of simulated radiation treatment. Imaging data from 10 different patients were categorized by important clinical markers, allowing multiple devices to be assessed in a single patient. Initial results showed variations in device treatment quality for different patient types, although a larger set of patients should be analyzed to assess these results.

15. SUBJECT TERMS
Monte Carlo Simulation, Medical Physics, Radiation, Brachytherapy, Breast Cancer

16. SECURITY CLASSIFICATION OF:			17. LIMITATION OF ABSTRACT	18. NUMBER OF PAGES	19a. NAME OF RESPONSIBLE PERSON
a. REPORT	b. ABSTRACT	c. THIS PAGE			19b. TELEPHONE NUMBER *(include area code)*
U	U	U	UU	12	

Table of Contents

Introduction

This project's dual objectives are the preparation of the PI for a career in breast cancer research and the design of a system of computer-base simulations capable of evaluating the effectiveness of various methods of breast cancer brachytherapy treatments both in general and for each individual patient for use in clinical decision-making. This will be achieved by developing a system that automatically generates models of patients using clinical data and allowing the user to explore various treatment options in the most realistic way possible, considering all physical interactions in order to accurately estimate and compare dose in any specific patient geometry for different devices. Once this is accomplished the system can be adjusted to be as close to real time as possible for ease of incorporation into treatment planning. The specific aims of the this project are:

SA0. Take the appropriate courses and acquire training to be become a professional Medical Physics researcher.

SA1. Develop Finite Element Method (FEM) tools to simulate the interaction between brachytherapy PBI devices and breast tissue.

SA2. Develop Monte Carlo Simulation (MCS) tools to estimate radiation dose distribution produced by a particular brachytherapy PBI device.

SA3. Compare the dosimetric features of all brachytherapy PBI devices for 10 breast cancer patients of various representative breast geometries using FEM and MCS tools developed in SA1 and SA2.

Body

I. Timeline

Activities		Year 1				Year 2				Year 3			
		Q1	Q2	Q3	Q4	Q1	Q2	Q3	Q4	Q1	Q2	Q3	Q4
Courses/Study	Cancer biology												
	Radiation biology												
	Radiotherapy Physics												
	Medical Imaging												
Clinical Skills	Delivery Methods												
	Treatment Planning												
	Special Procedures												
	Machine Commissioning												
	Machine Quality Assurance												
Laboratory Techniques	FEM												
	MCS												
	Parallel Computing												
	Software Development												

II. Courses/Study

SA0. Take the appropriate courses and acquire training to be become a professional Medical Physics researcher.

No additional courses were taken during this time.

III. Clinical Skills

During this year the PI shadowed clinical staff, observing and assisting in the brachytherapy treatment process from planning all the way to actual treatment of patients. During this time PI was trained on the BrachyVision™ treatment planning system with an emphasis on the new ACUROS software.

IV. Parallel Computing

The use of the Trestles cluster at the San Diego Super Computer center continued for both Monte Carlo and Finite Element Model applications.

V. Finite Element Model

SA1. Develop Finite Element Method (FEM) tools to simulate the interaction between brachytherapy PBI devices and breast tissue.

A. Device Modeling

Using manufacturer material and dimension specifications, models were developed for the three major breast-brachytherapy devices currently available: Mammosite®, Contura, and SAVI (figure 1) as well as interstitial catheters (Figure 2).

The devices began as simple geometrical approximations, including only the necessary parts. Interstitial catheters were the simplest being only a series of tubes. For the MammoSite and Contura devices, this included the center catheter, auxiliary catheters for the Contura and the balloon. For the SAVI this included the center catheter and surrounding struts as well as the constraint at each end that allows the device to expand. Parts were added incrementally in order to appropriately model and behavior the real devices while working within the complexities and constraints of the software. Any non-physical behavior such as unrealistic bending or materials and objects overlapping in space triggered adjustment to the model.

The balloons were be modeled by applying a uniform force of their surface area from the inside, thereby avoiding a computationally expensive fluid simulation while still closely mimicking their expected behavior when applied to breast tissue.

Of special interest was the superelastic/plastic behavior of Nitinol, which composes the struts of the SAVI and Contura devices. As the models of these devices, particularly the SAVI need to move realistically in order to determine the displacement and density change of the surrounding tissue, the struts needed to be modeled such that applied force would yield the correct deformation and consequently the proper shape.

Table 1

	Length (cm)	Width (cm)	Volume (cc)
MammoSite 4-5cm	4.00-4.65	4.00-5.10	34-77
MammoSite 5-6cm	5.11-5.73	4.87-5.90	70-125
Contura	4.75	4.50-6.00	40-100
SAVI 6 strut	5.50	3.00	15-30
SAVI 8 strut	6.00	4.00	30-60
SAVI 10 strut	6.50	5.00	60-90

Simulations of balloon and catheter devices exhibited expected behavior when force was applied to catheters (for the SAVI device and interstitial model) and when the balloon was inflated (for Mammosite® and Contura devices) meaning that the parts of the device moved in a realistic, physical manner when displacements of various points (range of length and width when inflated or expanded) as well as volume of the expanded device were compared to the actual measured dimensions of the devices (table 1). Simulated devices were considered valid if they could cover the range of dimensions within 10%.

B. Tissue Modeling

In order to create a realistic model of the patient including geometry and materials, voxel data from the TPS was imported into the FEM as a meshed geometry. Patient CT data post lumpectomy but prior to specific device insertion was used to establish a pre-device geometry.

Initially the patient model was intended to have a voxel by voxel tissue categorization from the CT data imported into the software. After several attempts to implement this, the PI found this technique to be untenable for two reasons: (1) CT data (unlike MR data) did not have the tissue density specificity necessary to distinguish between fatty and glandular tissue within acceptable limits (in addition to the problems created by device artifacts in the images) and (2) The number of necessary boundary conditions in the model in the FEM software if each voxel had a unique categorization proved too costly in the simulation phase.

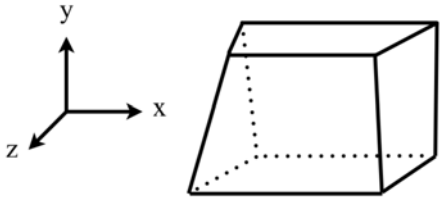

Figure 1: 8-node 3D mesh model for tissue.

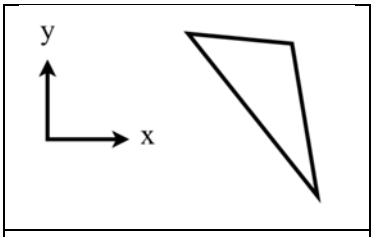

Figure 2: 3 node mesh model for skin.

A new strategy was used in which the boundaries of tissue and skin were dictated by the contours drawn in by a physician (already a normal part of the treatment planning process) and the tissue was then given one of the uniform material properties that were established in the simple model. In this scheme the tissue was decided by inspection to be either primarily fatty or primarily glandular with a separate tissue model for each of these options.

Using this technique, physician contours were imported to the FEM software and then meshed within the software, using eight node or tetrahedral mesh for the tissue and other internal structures and a triangular mesh for the skin (see figures 1&2).

SKIN

The mechanical properties of skin have been studied fairly extensively and there is a large body of work on the subject (Veronda and Westmann, 1970; Agache et al., 1980; Fung, 1981; Schneider et al., 1984). Although a heterogeneous material, for the forces used in our simulation the stress-strain relationship falls in the linear range. The standard experimental stress strain curve for skin (Elden, 1977) is can be approximated as a piecewise linear stress–strain curve which can be seen in figure 3.

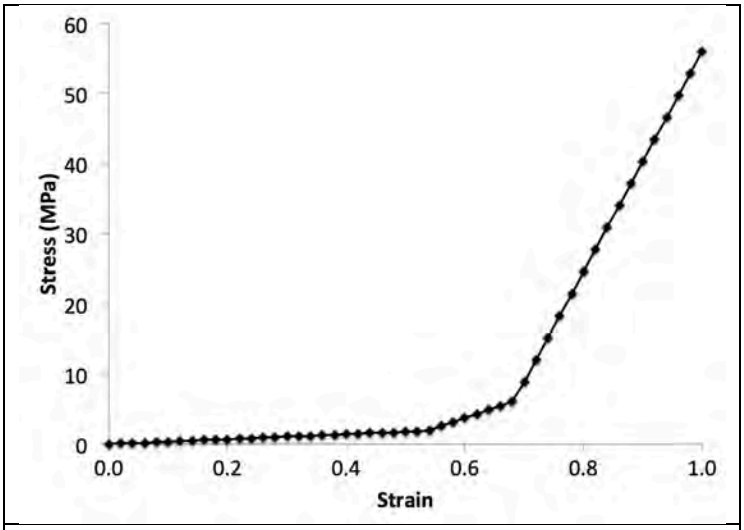

Figure 3: piecewise elastic modulus for skin.

Though it is not a homogeneous material, in many cases skin can be simplified to be statistically homogeneous (at higher strains it was found that the slope in the linear region of the stress–strain curve is similar in all directions) (Maurel et al., 1998). The typical experimental stress strain curve for skin (Elden, 1977) is transformed into a piecewise linear stress–strain curve which we will use to describe the mechanical properties of skin in the breast model (as shown in Fig. 8).

The stress-strain relationship used for skin is

$$\sigma_{skin} = A_i \cdot \varepsilon_{skin} + B_i$$

where A_i and B_i are the parameters the linear segments of the curve ($i = 1 - 3$) and the elasticity modulus is given by

$$E_{skin} = A_i (i = 1 - 3)$$

where there are three different parameters corresponding to a line segment which can be found in table 2.

Table 2

Parameter	Line segment 1	Line segment 2	Line segment 3
A_i (N/m^2)	3.43×10^6	2.89×10^7	1.57×10^8
B_i (N/m^2)	0	-1.36×10^6	-1.01×10^6
Strain range	$0 \le \varepsilon \le 0.54$	$0.54 \le \varepsilon \le 0.68$	$0.68 \le \varepsilon \le 1$

TISSUE

For the fat and glandular tissue model, exponential curves were used to describe the stress-strain relationship as they have been successfully for many different tissue types (Fung, 1993). The parameters for these curves were taken from measurements of fresh breast tissue within ten minutes of excision which were uniaxially loaded while being stored in a saline solution at room temperature (21±2.5°C) (Wellman and Howe, 1998). These curves can be fitted to the equation for elastic modulus E_n for tissue type n

$$E_n = \frac{\partial \sigma_n}{\partial \varepsilon_n} = b \cdot e^{m\varepsilon_n}$$

where σ_n and ε_n are the nominal stress and strain. Values for these parameters were taken from Azar and can be found in table 3. A Poisson's ratio of 0.49999 was used.

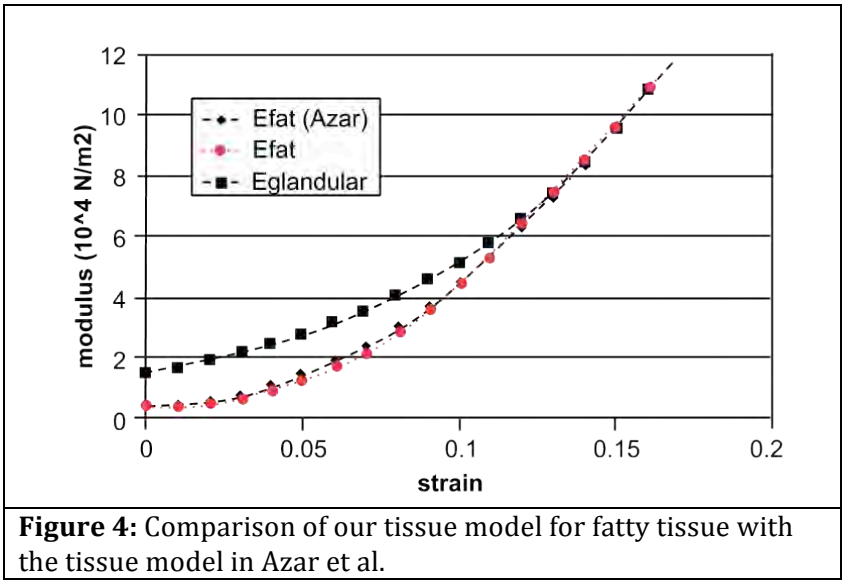

Figure 4: Comparison of our tissue model for fatty tissue with the tissue model in Azar et al.

Table 3

Parameter	Line segment 1
$b_{glandular}$ (N/m²)	15,1000
$m_{glandular}$	10
b_{fat} (N/m²)	4460
m_{fat}	7.4

C. Interaction of Device and Tissue Models

Once the tissue and device models have been developed, the different devices are simulated in each patient model. For this research, we used the SAVI, Contura and MammoSite device models described in section V, subsection A. Interstitial catheter models were omitted for the time being due to the difficulty in defining the boundary conditions to give satisfactory tissue deformation.

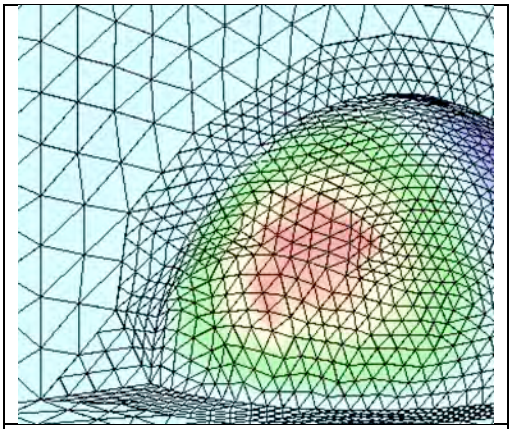

Figure 5: voxel map of Contura contour differences where red indicates difference close to 10% and blue is close to 0%.

In order to validate the FEM model, the FEM deformed contours were compared with the TPS contours created after real device insertion. This was done by both visual inspection and contour comparison. In order to measure the success of the FEM model, the contours had to be less than 10% displaced and the total volume of the cavity had to be within 3% of the real value. In addition to this any large visual discrepancies led to a reassessment of the mesh and boundary conditions of the model.

VI. Monte Carlo

SA2. Develop MCS tools to estimate radiation dose distribution produced by a particular brachytherapy PBI device.

A more accurate tissue model created for the Monte Carlo simulation, indicated that, while dose was still higher in the target region near the air-tissue interface, it was not as high as previously calculated.

Material and Methods

Data from TPS plans for 21 patients were used including CT image data, contoured structures and source information.

Phantom Description

CT images were imported into the PENELOPE code as voxel files where the various densities were determined by calibrated Hounsfield unit data from the CT scanner and the materials were determined by the contoured structures from the treatment plan. Four materials were used based on their distinguishability from each other due to the strength of their interaction with the 192Ir energies. (Bazalova et al.) These materials included tissue, air, bone and Nitinol.

Source Description

The source used was the VariSource 192Ir (Karaiskos et al.) with gamma and fluorescence x-rays from the NuDat database. Photons with intensity less than 0.1% and x-rays with energies below 10 keV were omitted as transmission of these through the 0.0125 cm nitinol capsule would be negligible (Casado et al.) and it saved a great deal of time in the simulation. The source model shown in figure 5 was created as a quadric structure consisting of a 10 mm long cylindrical capsule with semispherical ends and a diameter of 0.34 mm encased in wire 0.59 mm diameter also with a semispherical end. The wire extends 1 mm beyond the active core and 150 cm in the other direction. Only 1 cm is used in the simulation for simplicity, since there are many source dwell positions being simulated. In order to ensure that this did not affect the overall accuracy of the simulation, we compared dose differences between source models with different trailing wire lengths ranging from zero to twenty centimeters and found the difference anisotropy to acceptable (figure 6) with most of the dose difference landing within the wire itself, an area not counted when measuring the dose to a patient.

Source positions with orientations were extracted from the original plan. The positions were given in Cartesian coordinates and the orientation was determined using the tangent to the structural plot of each strut of the device (figure 7).

Monte Carlo

These simulations were run on the Trestles cluster at the San Diego Supercomputer Center using the 2008 PENELOPE software including penEasy and clonEasy packages. Each source position was run independently in the same phantom and then weighted according to its dwell time at that position before all simulations were summed voxel by voxel to find total dose. This was done with a voxel size of 0.6x0.6x0.6 mm. The simulation was set to generate histories until a sigma value of <0.5 was achieved. The average number of histories it took to achieve this was on the order of 10^9.

Actual Dose was calculated using the formula $D_i = A \cdot t \cdot f \cdot D_i^{MC}$ where D_i is the actual dose in eV/(g*histories), Ais activity in disintegrations/sec, t is time, and f is a calibration factor determined by comparing a simple source model MC simulation with one from the TPS.

Validation

In order to validate the accuracy of the simulation, a MC simulation of single source in water was compared to both to a TPS simulation of a single source in water and to results from a prior publication [2] of a single source in both water and water with an air cavity both using MC and ion chamber data.

TPS

For comparison of the single source in water done via MC and TPS, a 30x30x30 cm water phantom was used with voxel size was 0.6x0.6x0.6 mm. 2.3x10^9 histories were run and the results were compared with corresponding TPS results.

Literature
For comparison with MC and ion chamber data a phantom was created to simulate a ten-strut device containing an air cavity in a cylindrical water phantom 40 cm tall with a radius of 20 cm see figure 8). Voxel size was 2x2x2 mm and aproximately 1.7x10^9 histories were run for each simulation. The simulation was run with and without the air cavity.

Results
Validation
TPS
The TPS was used to test and calibrate the source model. The shape of the isodose lines matched well with the TPS results and the dose was close to the calculated dose when calibrated for activity. Plotting the isodose lines for the TPS versus the source model as seen in figure 9 shows the similarity of the results from the MC source model to the TPS results including symmetry and anisotropy. Subtraction analysis of the two doses (where dose is compared voxel by voxel) gives an average different of 0.1% and a maximum difference of 0.78% where the uncertainty value for the simulation is 0.4%.

Literature
Comparison to the model from Richardson et al can be seen in figure 10. The simulation yields similar results to Richardson et al. although our MC results are closer to their ion chamber results, particularly since there is no dropoff near the edge of the balloon for the MC simulation.

Monte Carlo
Isodose Line Analysis
Dose from the Monte Carlo plan was compared with dose from the original plan using isodose lines at 50, 100, 150 and 200% of the prescription dose of 34Gy. The lines were then plotted on the patient phantom in order to compare

Dosimetric Coverage
Dosimetric coverage of the target was also compared by evaluating the V150 and V200 (volume of the target covered by 150 and 200% of the dose respectively) and the V100 (percent of the target covered by 100% of the dose). The V150 and V200 had an average increase (and standard deviation) of 3.8% (1.4%) and 9.1% (3.2%) respectively, while the average change in V100 was 1.2% (1.0%).

Uncertainty Analysis
Although on average 2*10^10 histories were run for each full simulation in relatively small voxels, the variance was 0.9% which, while acceptable for most MC, introduces relatively large variations when comparisons, ratios or absolute differences are computed.

VII. Incorporation of Finite Element Model with Monte Carlo

SA3. Compare the dosimetric features of all brachytherapy PBI devices for 10 breast cancer patients of various representative breast geometries using FEM and MCS tools developed in SA1 and SA2.

The data of ten patients from the FEM model were imported back into the MC simulation in order to calculated dose for three different devices in the same patient. These 10 patients were chosen for comparison because they all had similar tumor bed volumes, meaning they all used the same size devices. Data was transformed from mesh back to voxel with structures determined by the FEM boundary conditions. The MC simulation followed the protocol addressed in the previous section, which addresses only the SAVI device, which is the most complex and computationally expensive simulation of the three. The results of these simulations were compared using a few key clinical metrics. Dose was observed in four critical volumes: the evaluated planning target volume (PTVeval), skin, ribs and lungs.

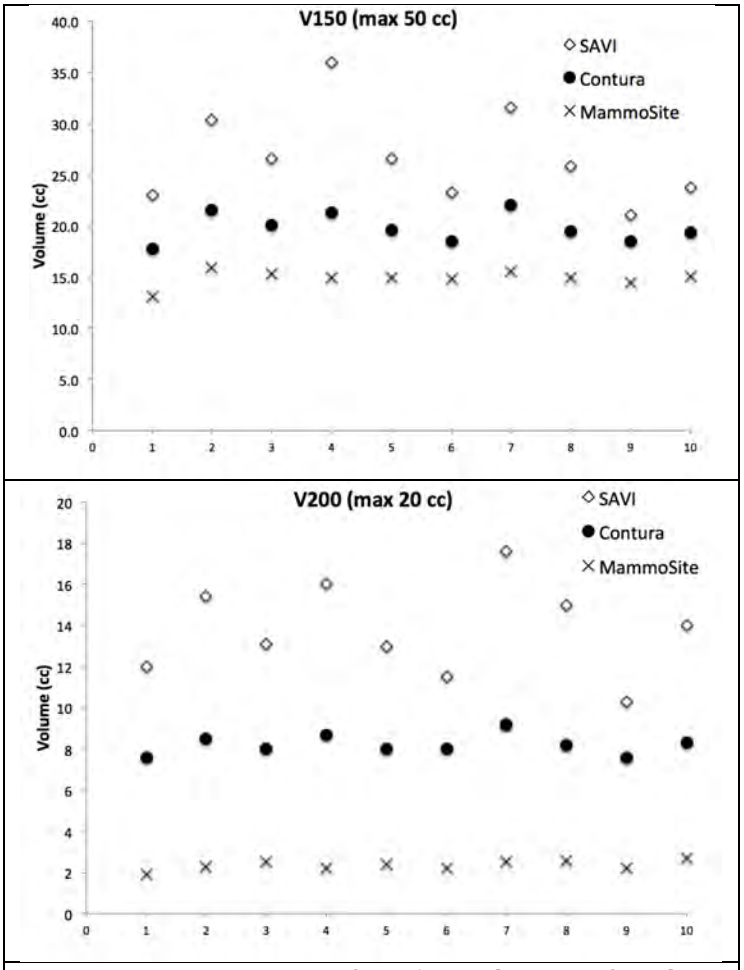

Figure 6: comparison of V150 and V200 for three devices in 10 different patients.

The evaluated planning target volume, or PTVeval, is calculated as one centimeter outside the cavity minus the cavity itself, the skin and the chest wall. The standard treatment is defined such that in this volume, at least 90% of should receive at least the prescription dose of 340 cGy while keeping volumes receiving over 150% of the dose below 50cc and volumes receiving over 200% of the dose under 20cc for interstitial catheter-type treatments and below 10% for balloon-type treatments. Using these criteria, simulations were run using the MC simulation after plan optimization using the original TPS. For the ten patients simulated with sufficient coverage of the PTVeval (V90 of 97.2% for SAVI, 95.7% for Contura and 93.1% for MammoSite) it was found that sufficient parameters could be reached for the V90, V150 and V200 values there was a trade off between dose to vital structures (skin, ribs and lungs) and dose homogeneity/ large V150 and V200 values.

In order to better understand the optimal use of each device on a personalize basis, a significantly larger number of patients should be compared.

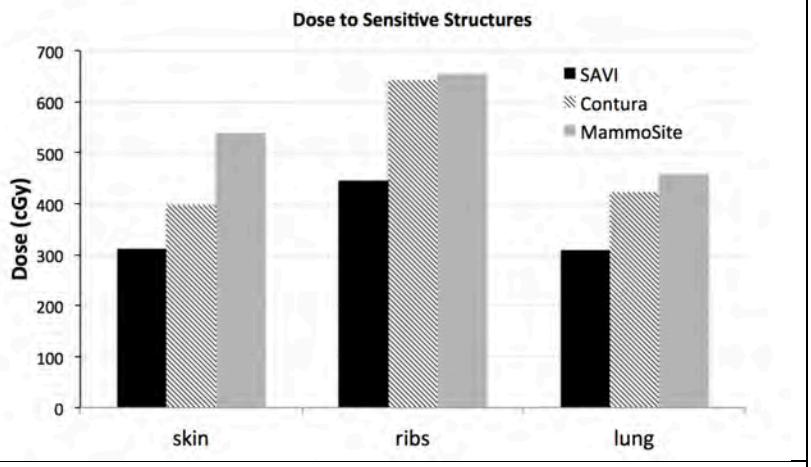

Figure 7: dose to sensitive structures for three different devices.

Key research accomplishments

- Successful development of a satisfactory tissue model for FEM.
- Simulation and comparison of multiple devices in a realistic patient geometry for both implantation and treatment.

Reportable outcomes

1. Grant Extended: Additional 25,000 SUs on the Trestles Cluster at the San Diego Super Computer Center.

Conclusions

In conclusion, the tissue model proved more difficult than anticipated resulting in many failed attempts before an acceptable model was achieved. The successful model led to 10 patient geometries given a comparative treatment using three different devices with results comparable to clinical data. In order to generate sufficient data to draw further conclusions about the comparison of multiple devices in the same patient, more patient data must be input and analyzed. PI continues to work on this project.

References

P G Agache, C Monneur, J L Leveque, J DeRigal, 1980. Mechanical properties and Young's modulus of human skin in vivo. Arch. Dermatol. Res. 269, 221–232.

F Azar, D Metaxas, M Schnall, A Deformable Finite Element Model of the Breast for Predicting Mechanical Deformations under External Perturbations. Journal of Academic Radiology (Oct. 2001)

F Azar, D Metaxas, M Schnall, Methods for modeling and predicting mechanical deformations of the breast under external perturbations, Medical Image Analysis, Volume 6, Issue 1, March 2002, Pages 1-27.

M Bazalova, E Graves, The Importance of Tissue Segmentation for Dose Calculations for Kilovoltage Radiation Therapy, Med. Phys. **38**, 3039 (2010).

Y C Fung, 1981. In: Biomechanics: Mechanical Properties of Living Tissues. Springer, New York, pp. 203–212.

Y C Fung, Biomechanics: Mechanical Properties of Living Tissues, Springer, Jun 18, 1993.

S Richardson, R Pino, Dosimetric Effects of an air cavity for the SAVI^{TM} partial breast irradiation applicator, Med. Phys. **37**, 3919 (2010).

D C Schneider, T M Davidson, A M Nahum., 1984. In vitro biaxial stress–strain response of human skin. Arch. Otolaryngol. 110, 329– 333.

D Veronda, R A Westmann, 1970. Mechanical characterization of skin-finite deformations. J. Biomech. 3, 111–124.

P S Wellman, R D Howe, 1998. Harvard Bio-Robotics Lab.Tech. Report. [98-121].

A Monte Carlo investigation of the dosimetric characteristics of the VariSource 192Ir high dose rate brachytherapy source.Karaiskos P, Angelopoulos A, Baras P, Sakelliou L, Sandilos P, Dardoufas K, Vlachos L. Med Phys. 1999 Aug;26(8):1498-502.

National Nuclear Data Center Decay Radiation database <http://www.nndc.bnl.gov/nudat2/>.

Francisco Javier Casado, Salvador García-Pareja, Elena Cenizo, Beatriz Mateo, Coral Bodineau, Pedro Galán, Dosimetric characterization of an 192Ir brachytherapy source with the Monte Carlo code PENELOPE, Physica Medica, Volume 26, Issue 3, July 2010, Pages 132-139, ISSN 1120-1797, 10.1016/j.ejmp.2009.11.001. (http://www.sciencedirect.com/science/article/pii/S1120179709000660)